A Framework for Determination of Heart Valves' Mechanical Properties Using Inverse-Modeling Approach

Ankush Aggarwal(✉) and Michael S. Sacks

Center for Cardiovascular Simulation, Institute for Computational Engineering and Sciences, Department of Biomedical Engineering, University of Texas at Austin, Austin, TX 78712, USA
ankush@ices.utexas.edu

Abstract. Heart valves play a very important role in the functioning of the heart and many of the heart failures are related to the valvular dysfunctions, e.g. aortic stenosis and mitral regurgitation. Relationship between the biomechanical properties of valve leaflets and their function has long been established, however, determining these properties in a non-invasive manner remains a challenge. Here we present a framework for such a tool for biomechanical properties determination. We use an inverse-modeling approach, where the only input is through imaging the leaflet tissue as it is loaded naturally during its functional cycle. Using a structural model for the leaflet material behavior allows us to reduce the number of parameters to be determined to only two, which in addition to dramatically reducing the computational time also allows one to visualize the cost function and the minimization process. We close with discussion about the contributions of the current framework and other constituents needed to make it a clinically viable tool.

1 Introduction

Heart valves are critical components of heart because of their role in ensuring the controlled flow of blood synchronized with the contraction of ventricles. The valve leaflets are complex, membrane-structural entities primarily made of collagen, elastin, extracellular matrix and cells. Either due to congenital defects or due to the changes due to remodeling with age, the leaflets functionality is altered sometimes resulting in less efficient heart output. Such problems are hard to diagnose at an early stage and may lead to heart failure if left untreated. Therefore, a tool for determining the functional properties of heart valves from non-invasive imaging modalities will be of utmost clinical importance. Such a tool will help diagnose valve diseases at an early stage as well as provide tools for monitoring the performance of replaced prosthetic valves. The three major components of such a tool are shown in Fig. 1. In order to define the correct reference configuration, we need the pre-strain information about leaflets. For defining the unknown fiber architecture, we need the population average architectures that can be used to constrain parameter optimization. Also, the proper choice of

H. van Assen et al. (Eds.): FIMH 2015, LNCS 9126, pp. 285–294, 2015.
DOI: 10.1007/978-3-319-20309-6_33

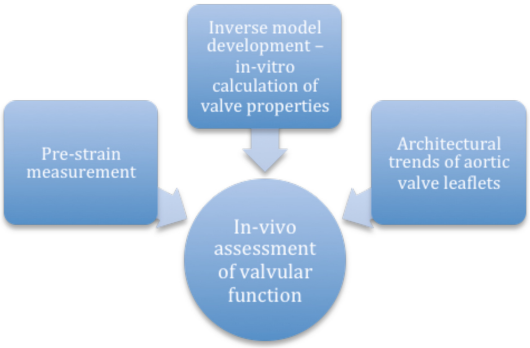

Fig. 1. Three components for an in-vivo assessment tool are pre-strain measurement, inverse model and population average fiber architecture of valve leaflets

constitutive model is important to best exploit fibrous structural information. Finally, the most critical component is development of a numerical inverse-model, which can be applied to in-vivo imaging data. In this paper, we focus on the development of inverse model using an in-vitro dataset and briefly discuss the other components.

2 Methods

To demonstrate the ideal capabilities of our approach, we utilized archival quality in-vitro experimental data from pericardial bioprosthetic heart valve to develop the parameter estimation tool based upon inverse modeling. The leaflets were imaged at three different static transvalvular pressures using surface markers and dual-camera setup [1] (Fig. 2). Leaflets were then removed and their fiber architecture was determined using light scattering technique [2]. Then the leaflets were dissected and put under biaxial test to determine their stress-strain relationship. This highly comprehensive data set with high resolution, marker positions at multiple pressures, valve specific fiber architecture and biaxial data was ideal for this study – to design the inverse model, validate it and calculate its sensitivity to various input parameters and optimization constraints. There is no existing method for inverse modeling of heart valves as per authors' knowledge. This is due to the difficulty in modeling them as well as their small size and thickness and fast movement in-vivo, leading to poor quality of imaging.

2.1 The Forward Model

Each of the valve leaflet was modeled as a thin shell and the contact between leaflets was treated using the augmented Lagrange multiplier method. The basal attachment was fixed as in the experiments and a normal pressure on the leaflets was applied linearly increasing upto 120 mm of Hg. The forward model was implemented in FEBio [3] using quadrilateral shell elements using quasi-static solver.

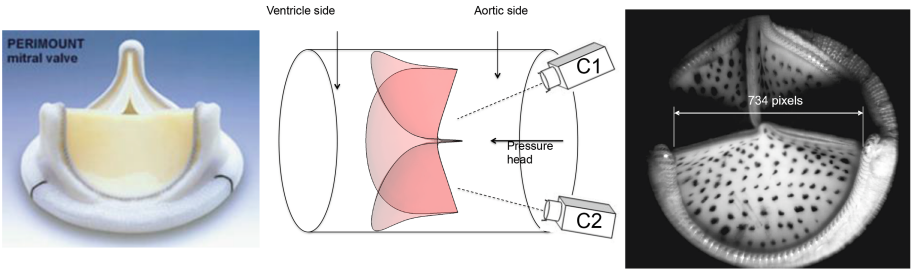

Fig. 2. The experimental setup to obtain valve shape in-vitro at different transvalvular pressure levels

The shape of the valve was provided by Edwards in the form of a quadrilateral meshed geometry file, where each leaflet was made up of 1025 cells and 1082 nodes. To improve the refinement as well as quality of elements, the geometry was imported into Hypermesh and remeshed with each leaflet made up of 2789 cells and 2880 nodes. Leaflets were discretized using four node quadrilateral elements, with each node assigned six degrees of freedom (three for translation and three for rotation). Therefore, the complete discrete version of the model had 51,840 degrees of freedom. A constant thickness was assigned to each leaflet as measured during the experiment. The stresses were integrated through the shell thickness using 3 point Gauss quadrature rule to obtain bending moments. To map the fiber architecture from two-dimensional output of the above-mentioned experimental method onto the three-dimensional valve structure, a spline-based technique previously developed was used [4].

2.2 The Material Model

The valve tissues are made up of multiple layers (fibrosa, ventricularis etc.) with different types of fibers embedded in a matrix for each of them [5,6]. However it is very hard to take into account the contribution of each layer separately. Therefore, here we take one of the most realistic material models developed – where tissue is idealized as a planar network of collagen fibers (main load bearing component) embedded in a ground substance (glycosaminoglycans, elastin, water) [7]. Thus, the strain energy is assumed to be a sum of the contributions from fibrillar (anisotropic) and non-fibrillar (isotropic) components expressed in terms of the tissue level Green-Lagrange strain $\mathbf{E}$:

$$\psi = \psi^{\mathrm{M}}_{\mathrm{iso}}(\mathbf{E}) + \psi^{\mathrm{F}}_{\mathrm{aniso}}(\mathbf{E}). \tag{1}$$

Here $\psi^{\mathrm{M}}_{\mathrm{iso}}$ and $\psi^{\mathrm{F}}_{\mathrm{aniso}}$ are strain energy functions representing ground-matrix and fiber contributions respectively. The ground-matrix function describes low-strain behavior and provides stiffness in the unloaded state. Tissue response to large strains is accommodated by the anisotropic term characterizing the fibrillar microstructure averaged through the thickness. The isotropic contribution is

assumed to be neo-Hookean. Following the formulation in [7], the ensemble 2nd Piola-Kirchhoff stress in a single fiber is

$$S_{\text{ens}}\left(E_{\text{ens}}\right) = \frac{\partial \psi_{\text{ens}}}{\partial E_{\text{ens}}} = \eta \int_0^{E_{\text{ens}}} D(x) \frac{E_{\text{ens}} - x}{(1+2x)^2} dx \tag{2}$$

where, η is the fiber stiffness, D is the fiber recruitment function and E_{ens} is the uniaxial Lagrangian strain in single fiber aligned in direction $\boldsymbol{N}$ so that $E_{\text{ens}} = \boldsymbol{N}\cdot\mathbf{E}\cdot\boldsymbol{N}$. However, in present formulation, to avoid extremely high computational times, a simplified model was used [8], where the integral is approximated as an exponential function:

$$S_{\text{ens}}\left(E_{\text{ens}}\right) = A(e^{BE_{\text{ens}}} - 1) \tag{3}$$

The important aspect of this approach is that it allows us to reduce the number of unknown material parameters in fiber component to only two, thus, reducing the computational time in determining them. The matrix component was modeled as a compressible neo-Hookean material and the properties were borrowed from flexural testing results previously published. For a distribution of fibers in a planar biaxial state, we get the planar stress by integrating over the distribution

$$\mathbf{S}^{\text{F}}_{\text{aniso}}\left(\mathbf{E}\right) = \frac{\partial \psi^{\text{F}}_{\text{aniso}}}{\partial \mathbf{E}} = \int_{-\pi/2}^{\pi/2} R\left(\theta\right) S_{\text{ens}}\left(\boldsymbol{N}\cdot\mathbf{E}\cdot\boldsymbol{N}\right) \boldsymbol{N}\otimes\boldsymbol{N} d\theta \tag{4}$$

The fiber distribution $R(\theta)$ was determined at every point of the tissue using SALS setup [2] and approximated as a normalized Gaussian distribution. For the matrix part $\psi^{\text{M}}_{\text{iso}}$, a neo-Hookean model was used for which there parameters were estimated from flexural studies previously conducted.

2.3 The Algorithm

The above forward model was put in an optimization loop where the parameters were initialized with a guess and solution was iterated until convergence was achieved. The objective cost function was defined as the difference in shape of the deformed mesh and that of the experimental data points. The difference was calculated along the normal direction of deformed mesh. Thus, it can be defined mathematically as

$$\mathcal{F} = \sqrt{\sum_{i,\alpha} \left(x_i^\alpha - \tilde{x}_i^\alpha\left(c_m\right)\right)^2} \tag{5}$$

where, x_i^α are the input points from experiment and $\tilde{x}_i^\alpha$ are their projection on deformed valve surface obtained from the forward model with material parameters c_m. It should be noted that the above cost function does not use the information about experimental data points being the material points. Instead,

the points were used only to describe valve shape. This was done to be consistent with the clinical imaging modalities (e.g. ultrasound) which provides only the shape without any information about material points. The minimization of above defined cost function is a highly non-linear function because of the contact constrained between leaflets. The non-linear least squares problem of minimizing the cost function was solved using Levenberg-Marquardt algorithm:

$$\mathbf{J}^T\mathbf{J} + \lambda \text{diag}(\mathbf{J}^T\mathbf{J}))\Delta c_m = \mathbf{J}^T\left(x_i^\alpha - \tilde{x}_i^\alpha\left(c_m\right)\right), \tag{6}$$

where derivatives of the cost function $\mathbf{J} = \partial \tilde{x}_i^\alpha\left(c_m\right)/\partial c_m$ were calculated numerically using central difference method by perturbing each of the parameters 1 % above and below its current value. The value of λ was kept constant a value of 5 since it provides a balance between the stability and convergence speed of the algorithm. The simulations were run on Texas advanced computing center (TACC) on a single node with 12 processors. The finite difference cases for cost function derivatives were run in parallel using multiprocessing module of python wrapper. For n parameters, this setup required a total of $2n + 1$ simulations in parallel. Each iteration of the inverse model approximately took 35–40 min.

3 Results

Our approach allows the entire problem to be reduced to optimization of just two parameters; with the cost function shape for various cases as a function of the two material parameters A and B is shown in Fig. 3. The results demonstrate the importance of using higher number of frames from in-vivo imaging for inverse modeling input. It also shows that imaging at higher pressures would give a better confidence in the results. It is also noted that the cost function is almost convex everywhere. However, the lowest part of the cost function is a long banana-shaped region instead of a single point. This is a property of the exponential form of the ensemble response function and can be analyzed analytically (see Appendix). Similar behavior of the exponential function has been previously reported in inverse modeling of myocardium [9]. The closed-form equation for the lowest region Eq. 9, which we will refer to as the "iso-stress-strain minima" region, thus obtained can also be used to reduce the number of parameters in the optimization process in the future. Furthermore, it is noted that the minima of the cost function resembles the error function from biaxial testing. This signifies that although the valve is loaded under normal pressure, locally it still behaves like a planar membrane under biaxial load.

Using the current approach, it is also possible to evaulate sensitivity of results to various input parameters. The change in cost function when average fiber architecture is utilized is shown in Fig. 4a and when it is varied the result is shown in Fig. 4b. This result demonstrates that the inverse modeling results are dependent upon the fiber architecture in an average sense. The results were found insensitive to the Poisson's ratio of the matrix, but highly sensitive to the noise in input point cloud from imaging (Fig. 5). Statistics of the final fit are shown in Table 1. Comparison of predicted stress-strain relationship vs. measured are

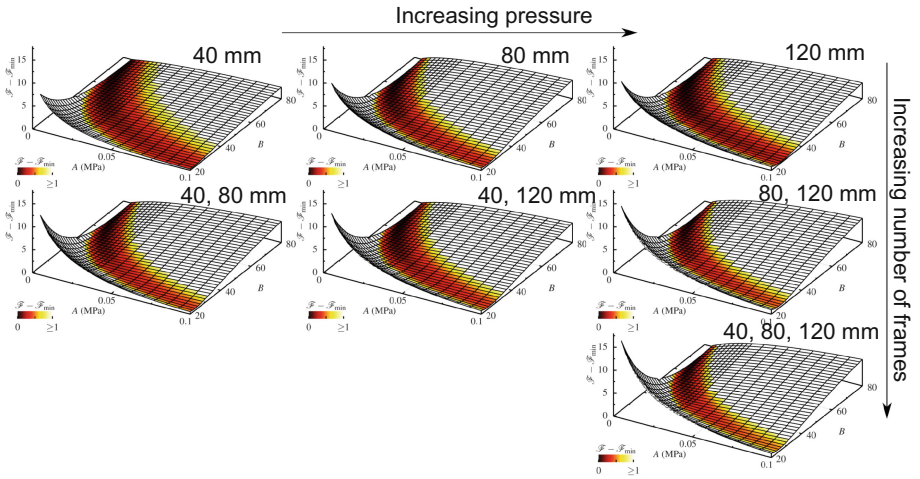

Fig. 3. Cost function using various pressure levels and various number of frames

shown in Fig. 6a and the final fit of valve's deformed shape to point cloud is shown in Fig. 6b. Our framework was able to obtain an excellent fit of the final deformed shape to marker positions. However, there is a small difference in the effect stress-strain response when compared with the biaxial data. The differences could be attributed to multiple factors, but we believe the discrepancy is predominantly due to the effect of preconditioning. Preconditioning is a part of the standard biaxial experiment protocol and was also used for obtaining the experimental results in the current setup. However, its effect is not entirely understood and one could argue that the leaflets were not preconditioned before loading the valve under static pressure head. Additionally, the material models for soft tissues are usually not sufficient for extrapolation of results. Since the strain path employed during biaxial tests is sufficiently different from those during the natural loading of valve, some differences can be expected. The importance of present results and its possible extension to become a viable clinical tool are discussed next.

4 Discussion

Biomechanical properties of heart valve leaflets play an important role in determining their durability as well as susceptibility to disease development. Abnormal mechanical behavior leads to changes in the stress state of VICs and, eventually causing them to adopt a pathological phenotype. Therefore, changes in the mechanical properties of valve leaflets during their lifetime could be used an indicator for pathological functionality. However, the current methods for determining biomechanical properties are limited by their need for an excised valve leaflet. Therefore, a tool that could be used for going from in-vivo imaging to mechanical properties of the valve will be very useful. Additionally, such a

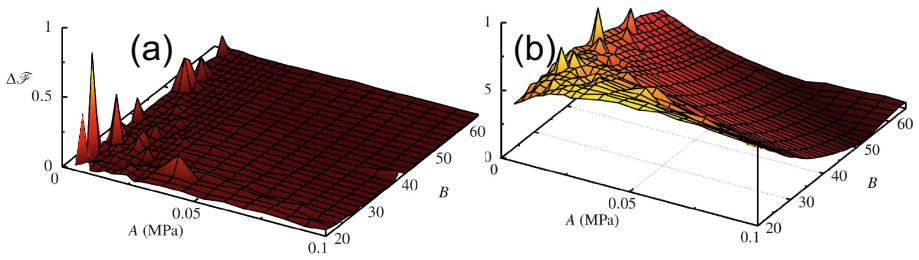

Fig. 4. Changes in cost function due to variation in fiber splay: (a) using average value of 0.58 rad and (b) using a value of 0.5 rad

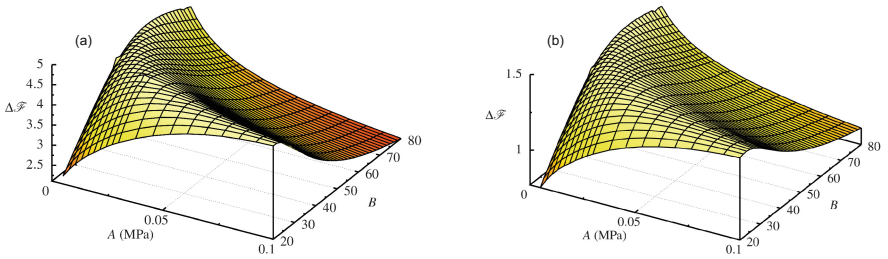

Fig. 5. Changes in the cost function due to noise in the input data – uniform/systematic noise (a) and random Gaussian noise with standard deviation of 0.2 mm (b)

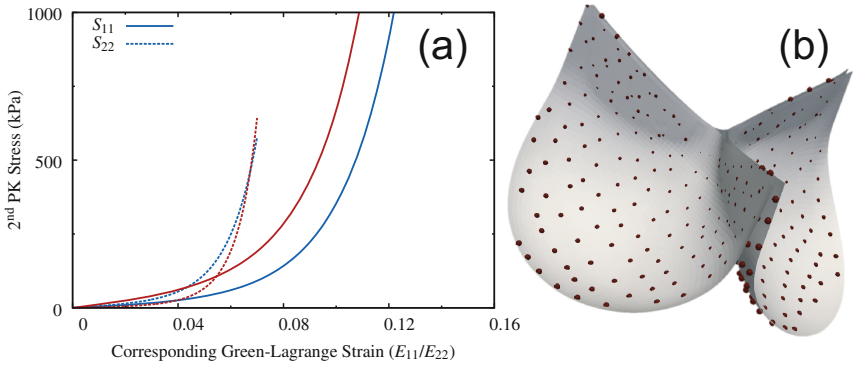

Fig. 6. (a) Comparison of stress-strain response from experiment and inverse model. (b) The final fit to the point cloud using current framework.

tool will also be useful in determining the causes of failure of prosthetic valves, and help us improve their designs in the long run.

The framework developed in this paper presents an approach for inverse model development for heart valves exploiting mapped leaflet structures. Herein each leaflet is considered to have homogenous elastic parameters. The novelty of the present work lies in the incorporation of mapped fiber data of each leaflet

Table 1. Statistics of the final fit

Pressure	Leaflet	mean($\|d\|$)	std($\|d\|$)	max($\|d\|$)
40 mm	1	0.195	0.150	0.718
40 mm	2	0.238	0.196	0.977
40 mm	3	0.182	0.124	0.619
80 mm	1	0.214	0.169	0.786
80 mm	2	0.294	0.232	1.150
80 mm	3	0.199	0.140	0.574
120 mm	1	0.270	0.216	0.938
120 mm	2	0.270	0.238	1.155
120 mm	3	0.196	0.137	0.611

and utilizing it through simplified structural model [8]. Differences in fiber architectures of normal and pathological valve leaflets previously determined [4] can be combined with this tool to predict abnormal biomechanical behaviors. The sensitivity and convergence studies provide guidelines for creating this tool in an effective manner, e.g. the imaging resolution is a critical component of accurate determination, and higher number of frames leads to higher confidence.

To develop a method for evaluating the material parameters from in-vivo imaging, we are also working on other required components. The average fiber architecture of valve leaflets was calculated using a novel spline technique [4] and the pre-strain in leaflets was estimated by comparing the in-vivo shape and explanted leaflets' shape [10]. This information when combined with the inverse model presented in this work will lead to an in-vivo assessment tool for heart valves. Such a tool will help determine the mechanical properties of heart valves and find relations to disease development and help diagnose problems in the mechanical functionality at an early stage. Additionally, this approach will have the potential to serve as a general-purpose in-vivo assessment tool for heart valves for evaluating the performance of replaced prosthetic valves as well as monitoring the progression of valve diseases. In future, the method will be extended for the parameters to vary spatially. The information thus produced over time will help us understand the mechanical behavior of valve leaflets and design better surgical tools to repair and replace them.

Acknowledgment. We gratefully acknowledge the help from Will Zhang with parameter estimation and analysis of biaxial data. This work was supported by NIH Grant HL108330 and Moncrief Chair funds (M.S.S.) and American Heart Association Postdoctoral Fellowship 14POST18720037 (A.A.). The authors acknowledge the Texas Advanced Computing Center at The University of Texas at Austin for providing HPC resources.

Appendix

Exponential function of the form $f(A, B, x) = A(e^{Bx} - 1)$, where $x \in \mathbb{R}^+$ is the independent variable, is very common in soft tissue mechanics to describe the stress-strain behavior so that its stiffness increases linearly with stress. Here $A \in \mathbb{R}^+$ and $B \in \mathbb{R}^+$ are the material parameters that determine the quantitative nature of this function or stress-strain relationship. However, many different pairs of (A, B) values can give very similar responses. To analyze this aspect, we first construct a functional that calculates the difference between two functions with different set of parameters:

$$\mathcal{F}(A, B, \bar{A}, \bar{B}, \epsilon) = \int_0^{\epsilon} \left[A(e^{Bx} - 1) - \bar{A}(e^{\bar{B}x} - 1)\right]^2 dx. \tag{7}$$

$\epsilon \in \mathbb{R}^+$ is the upper strain limit for a given application. To find the curve in $A-B$ parameter space along which the function $f(A, B, x)$ is "closest" to $f(\bar{A}, \bar{B}, x)$, we minimize the functional $\mathcal{F}$ for a given B, i.e.

$$\underset{A\in\mathbb{R}^+}{\arg\min}\, \mathcal{F}(A, B, \bar{A}, \bar{B}, \epsilon) = \underset{A\in\mathbb{R}^+}{\arg\min} \int_0^{\epsilon} \left[A(e^{Bx} - 1) - \bar{A}(e^{\bar{B}x} - 1)\right]^2 dx = A^{\min}(B, \bar{A}, \bar{B}, \epsilon) \tag{8}$$

One can obtain a closed form solution under reasonable conditions (which are satisfied if $\epsilon \leq 1$, something usually true for strain):

$$A^{\min}\left[g(2B) - 2g(B) + 1\right] = \bar{A}\left[g(B + \bar{B}) - g(B) - g(\bar{B}) + 1\right], \tag{9}$$

where,

$$g(B) = \frac{e^{B\epsilon} - 1}{B\epsilon}. \tag{10}$$

References

1. Sun, W., Abad, A., Sacks, M.S.: Simulated bioprosthetic heart valve deformation under quasi-static loading. J. Biomech. Eng. **127**(6), 905–914 (2005)
2. Sacks, M., Smith, D., Hiester, E.: A small angle light scattering device for planar connective tissue microstructural analysis. Ann. Biomed. Eng. **25**(4), 678–689 (1997)
3. Maas, S.A., Ellis, B.J., Ateshian, G.A., Weiss, J.A.: Febio: finite elements for biomechanics. J. Biomech. Eng. **134**(1), 011005 (2012)
4. Aggarwal, A., Ferrari, G., Joyce, E., Daniels, M.J., Sainger, R., Gorman III, J.H., Gorman, R., Sacks, M.S.: Architectural trends in the human normal and bicuspid aortic valve leaflet and its relevance to valve disease. Ann. Biomed. Eng. **42**(5), 986–998 (2014)
5. Sacks, M., Yoganathan, A.: Heart valve function: a biomechanical perspective. Philos. Trans. Royal Soc. B: Biol. Sci. **362**(1484), 1369–1391 (2007)

6. Sacks, M., David Merryman, W., Schmidt, D.: On the biomechanics of heart valve function. J. Biomech. **42**(12), 1804–1824 (2009)
7. Sacks, M., et al.: Incorporation of experimentally-derived fiber orientation into a structural constitutive model for planar collagenous tissues. J. Biomech. Eng. **125**(2), 280 (2003)
8. Fan, R., Sacks, M.S.: Simulation of planar soft tissues using a structural constitutive model: finite element implementation and validation. J. Biomech. **47**(9), 2043–2054 (2014)
9. Xi, J., Lamata, P., Niederer, S., Land, S., Shi, W., Zhuang, X., Ourselin, S., Duckett, S.G., Shetty, A.K., Rinaldi, C.A., Rueckert, D., Razavi, R., Smith, N.P.: The estimation of patient-specific cardiac diastolic functions from clinical measurements. Med. Image Anal. **17**(2), 133–146 (2013)
10. Aggarwal, A., Aguilar, V.S., Lee, C.H., Ferrari, G., Gorman, J.H., Gorman, R.C., Sacks, M.S.: Patient-specific modeling of heart valves: from image to simulation. In: Ourselin, S., Rueckert, D., Smith, N. (eds.) FIMH 2013. LNCS, vol. 7945, pp. 141–149. Springer, Heidelberg (2013)